

BULETINUL INSTITUTULUI POLITEHNIC DIN IAȘI
Publicat de
Universitatea Tehnică „Gheorghe Asachi” din Iași
Volumul 64 (68), Numărul 3, 2018
Secția
CHIMIE și INGINERIE CHIMICĂ

**SYNTHESIS, CHARACTERIZATION AND BIOLOGICAL
ACTIVITY EVALUATION OF SOME DIVALENT
TRANZITIONAL METALS COMPLEXES
WITH N-p-NITROBENZOYL-D-L-PHENYLGLYCINE**

BY

**CĂTĂLINA ROȘCA¹, VALERIU ȘUNEL², MIHAELA CREȚU², MARIANA
DIACONU¹, DANIEL MARECI¹, CARMEN MÎȚĂ², CORNEL STAN¹,
GABRIELA ANTOANETA APOSTOLESCU¹ and DANIEL SUTIMAN^{1,*}**

¹“Gheorghe Asachi” Technical University of Iași, Romania,
“Cristofor Simionescu” Faculty of Chemical Engineering and Environmental Protection

²“Alexandru Ioan Cuza” University of Iași, Romania,
Faculty of Chemistry

Received: July 16, 2018

Accepted for publication: August 25, 2018

Abstract. This paper presents the synthesis of some Mn(II), Co(II), Ni(II) and Cu(II) complexes with N-p-nitrobenzoyl-D-L-phenylglycine (NBPG) as ligand. The characterization of the above mentioned synthesised compounds involved the structure determination by elemental analysis, FTIR spectroscopy, X-ray diffraction (XRD) and electron spin resonance (ESR). Experimental data sustain that all Mn, Co, Ni and Cu derivatives of N-p-nitrobenzoyl-D-L-phenylglycine present a crystalline structure framed orthorhombic system and are thermally stable up to temperatures above 100°C. The results of the toxicity tests on mice indicated that the lowest value of the lethal dose is displayed by the Cu complex compound. The antibacterial and antifungal activities investigations revealed that the Co[(L)₂(H₂O)₂] compound displays the best antibacterial properties while the Cu[(L)₂(H₂O)₂] compound presents the best antifungal properties.

Keywords: antibacterial and antifungal activity; divalent transitional metals complexes; ESR; FTIR; N-p-nitrobenzoyl-D-L-phenylglycine; XRD.

*Corresponding author; *e-mail*: sutiman@ch.tuiasi.ro

1. Introduction

Heterocyclic compounds have various applications in medicine and pharmacology due to their intrinsic biological properties in the human body or in other living organisms (Sperry and Wright, 2005; Strohl, 2000; Boxall *et al.*, 2006). Furthermore, antifungal (Wujec *et al.*, 2004; Zou *et al.*, 2002; Chen *et al.*, 2000) and antibacterial (Varvaresou *et al.*, 2000; Erol *et al.*, 2001; Pintilie *et al.*, 2007a) effects also, were reported.

Some amino acids or their derivatives with the capacity to donate electrons may be used as ligands for the synthesis of complex heterocyclic combinations, due to their functional groups capable of forming coordination bonds (Ryabov *et al.*, 1984; Inomata *et al.*, 1988; Salas Peregrin *et al.*, 1985; Gudasi *et al.*, 2007; Pelagatti *et al.*, 2005).

N-acylated amino acids being normally involved in the protein metabolism may ensure liver protection while acting as appropriate delivering agents for different antimicrobial or antifungal agents (Şunel *et al.*, 2002; Pintilie *et al.*, 2007b; Moise *et al.*, 2008; Şunel *et al.*, 2005; Şunel *et al.*, 2008).

These data generate the idea to obtain heterocyclic coordination compounds containing Mn, Co, Ni or Cu and N-p-nitrobenzoyl-D-L-phenylglycine as ligand (L) with potential lower toxicity and enhanced antimicrobial or antifungal activity.

This paper presents synthesis, structural characterization and thermal stability evaluation of some Mn(II), Co(II), Ni(II) and Cu(II) coordination compounds with N-p-nitrobenzoyl-D-L-phenylglycine as ligand (L). Ligand structure is shown in Fig. 1.

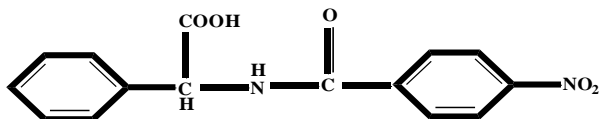


Fig. 1 – Structure of N-p-nitrobenzoyl-D-L-phenylglycine (L).

Furthermore, toxicity test, antimicrobial and antifungal activities were investigated for all above mentioned coordination compounds in order to evaluate their biological activity.

2. Materials and Methods

2.1. Synthesis of Metal (II) Complexes with N-p-Nitrobenzoyl-D-L-Phenylglycine (NBPG) as Ligand

The organic ligand was synthesized at 10-12°C by condensation reaction between chloride of p-nitrobenzoic acid (dissolved in anhydrous

benzene) with phenylglycine, in sodium bicarbonate solution. The product was purified by column chromatography on silica gel using a mixture of dichloromethane-methanol (9:2), as eluent (Pintilie *et al.*, 2006).

The complexes were synthesized by direct reaction of the ligand solution (0.1M) dissolved in ethanol with the metal chloride solution (0.1M) dissolved in water, mixed in a molar ratio of 2/1 and stirred at 50°C for 3 h. The final product was separated by slow crystallization at room temperature for several days, purified by recrystallization in ethanol and washed until the complete removal of Cl⁻ ion.

2.2. Structure Investigation and Thermal Stability Evaluation

2.2.1. Elemental Analysis

Elemental analysis of C, N, and H (by oxygen combustion) and O (by pyrolysis), on the Thermo Fisher Scientific equipment Flash EA-1112CHNS/O, was carried out in order to determine the structure of these compounds. Data acquisition and interpretation was performed with specialized software - Eager 300.

2.2.2. FTIR

FTIR analysis was performed on a Perkin-Elmer Spectrum 100 device, in the range 400-4000 cm⁻¹ (in KBr), aiming to evaluate the mainly changes in the group -COOH and R-NH ligand that binds to cation metal.

2.2.3. ESR

ESR spectra were performed on a device ESR CMS 8400 (3216.9 Gauss magnetic field corresponding to the centre of sample and 9030 MHz frequency). The spectroscopic splitting factor *g* and the odd number of electrons that returned each metal atom were determined using the standard diphenyl picryl hydrazine.

2.2.4. XRD

XRD analysis was performed on a device Holland X'Pert diffractometer PROMRD Panalytical (Cu K α radiation) in order to determine basic parameters and cell volume.

2.2.5. Thermal Stability

Thermal stability was analyzed on a Diamond TG / DTA (PerkinElmer) thermo-balance with a heating rate of 10°C min⁻¹ in the range 20-700°C.

2.3. Biological Activity

2.3.1. Toxicity Tests

Toxicity tests were evaluated based on the (LD₅₀) indicator representing the dose that kills 50% of the experimental animals. Groups of ten mice, both sexes, weighting 20±2 g were used. The synthesized compounds being insoluble in water, were suspended in Twen 80 and injected intraperitoneal on a daily basis. The mice were monitored for seven days and the LD₅₀ was determined according to the Spearman – Karber method (Hamilton *et al.*, 1977).

2.3.2. Antibacterial and Antifungal Activity

The antibacterial activities of the synthesized complexes against *Staphylococcus aureus* (RCMB-000106), *Bacillus subtilis* (RCMB-000108) as Gram positive bacteria and, *Escherichia coli* (RCMB-000103) and *Pseudomonas aeruginosa* (RCMB-000102) as Gram negative bacteria were screened using the agar well diffusion method (Rattan, 1999). The wells were made (by using a sterile metallic borer) with the centres at 20 mm at least. Eight – hour – old bacteria inoculums containing approximately 10⁶ colony forming units per millilitre (CFU/mL) were spread on the surface of the agar medium by using sterile cotton swabs. The compounds that were tested (2 mg·mL⁻¹ in sterile distilled water) were added into the respective wells. Other wells were supplemented with sterile distilled water as a positive control. The plates were incubated at 37°C for 20 h. Inhibition zone diameter in mm was used as criterion for the antimicrobial activity using the agar diffusion well method.

The antifungal activities of the synthesized compounds against two fungi species, *Candida albicans* (RCMB 05035) and *Aspergillus fumigates* (RCMB-002003), were tested by using the tube diffusion test (Rattan, 1999; Domer, 1971). Stock solutions of synthesized compounds (100 mg·mL⁻¹) were prepared in sterile distilled water. Sabouraud dextrose agar media (10 mL) was distributed into sterile tubes and autoclaved at 121°C for 15 min. Test compounds (10 mg·mL⁻¹) were added from the stock solutions to non -solidified media. After solidification at room temperature, the tubes were inoculated with 4 mm diameter portions of inoculums derivates from a seven day old fungal culture. A control tube (without test solutions) for each fungus strain was inoculated. All experimental tubes were incubated at 27°C for 5 – 7 days and the growth of tested fungi was determined by measuring the linear growth (in mm) in the test tubes and compared to the growing of fungus in control. The degree of growth inhibition was calculated as:

$$\text{Inhibition (\%)} = [(A-B)/B] \times 100$$

were: A – linear growth of the fungal colony in control tube; B – linear growth of the fungal colony in test tube.

3. Results and Discussion

3.1. Structure Evaluation

3.1.1. Elemental Analysis

Elemental analysis data are presented in Table 1. Theoretical calculation was made by considering the molecular formula: $M(L)_2(H_2O)_2$, deduced from M:L molar ratio and thermal analyses data, and the results of the experimental analysis indicates that all new synthesized compounds correspond to the above mentioned molecular formula.

Table 1
Theoretical and Experimental Chemical Composition of Synthesized Compounds

Complex with	% C		% N		% H		% O		% metal	
	Calc.	Exp.	Calc.	Exp.	Calc.	Exp.	Calc.	Exp.	Calc.	Exp.
Mn(II)	52.40	51.98	8.15	8.20	3.49	3.32	27.94	28.06	8.00	8.35
Co(II)	52.17	52.25	8.11	8.07	3.48	3.37	27.94	28.12	8.40	8.16
Ni(II)	52.12	52.03	8.15	8.21	3.47	3.52	27.80	27.83	8.50	8.37
Cu(II)	51.75	51.55	8.05	7.98	3.45	3.61	27.60	27.73	9.13	9.09

3.1.2. FTIR Spectroscopy

The infrared spectrum of the L ligand exhibits a sharp band at 3399 cm^{-1} assigned to O-H stretching vibration of COOH group, which disappeared after coordination (Fig. 2, Table 2), fact indicating that the carboxyl group interacted with the metal cation.

Table 2
Infrared Frequencies (cm^{-1}) and Assignments of Characteristic Absorption Bands for (1) L, (2) $[Mn(L)_2] \cdot 2H_2O$, (3) $[Co(L)_2] \cdot 2H_2O$, (4) $[Ni(L)_2] \cdot 2H_2O$ and (5) $[Cu(L)_2] \cdot 2H_2O$

(1)	(2)	(3)	(4)	(5)	Assignments
3399	3400	3401	3415	3478, 3420	$\nu(\text{OH})$ (COOH) $\nu(\text{OH})$ (H_2O)*
3115	3108	3080	3075	3060	$\nu(\text{NH})$ *
2949	2978	2980	2976	2985	$\nu(\text{CH})_{\text{methvlene}}$ *
1704	1693	1693	1693	1694	$\nu(\text{C}=\text{O})_{\text{amide I}}$
1664	1647	1649	1641	1649	$\nu_{\text{as}}(\text{COO})$
1541	1525	1526	1527	1526	$\nu_{\text{amide II}}$
–	1409	1407	1406	1412	$\nu_{\text{s}}(\text{COO})$
1207	1179	1178	1179	1178	$\nu(\text{C}-\text{O})$
1109	1107	1110	1111	1109	$\nu(\text{C}-\text{N})$

*determined by deconvolution of original spectra

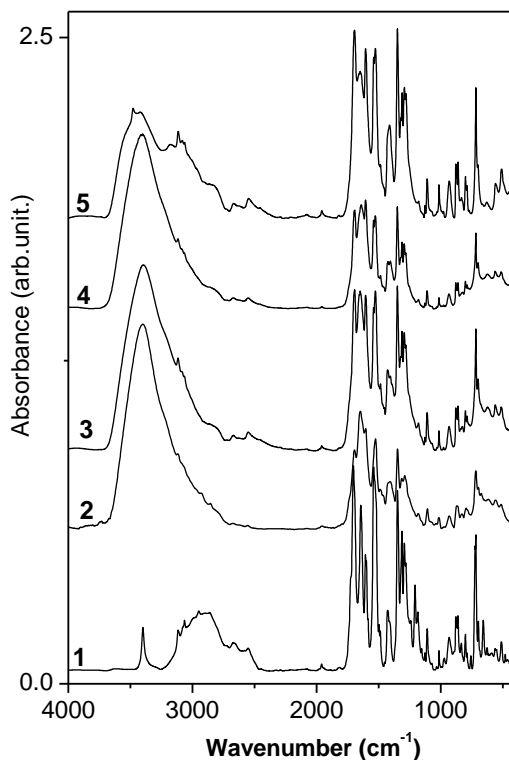


Fig. 2 – Infrared spectra of (1) L, (2) $[\text{Mn}(\text{L})_2] \cdot 2\text{H}_2\text{O}$, (3) $[\text{Co}(\text{L})_2] \cdot 2\text{H}_2\text{O}$, (4) $[\text{Ni}(\text{L})_2] \cdot 2\text{H}_2\text{O}$ and (5) $[\text{Cu}(\text{L})_2] \cdot 2\text{H}_2\text{O}$.

The FTIR spectra of Mn(II), Co(II), and Ni(II) and Cu(II) complexes from Fig. 2 are presenting all characteristic features of neutral complexes. The spectra of solid complexes shows a strong broad band in the $3500 - 3300 \text{ cm}^{-1}$ domain, fact that indicates the presence of water molecules. Lower intensity of $\nu(\text{O-H})$ band for $[\text{Cu}(\text{L})_2] \cdot 2\text{H}_2\text{O}$ complex can be explained by the difference between polarity of O-H bonds due to existence of intermolecular hydrogen bond between the water molecule and the oxygen atom that belongs to the C=O group of nearest $[\text{Cu}(\text{L})_2]$ molecule.

The thermal decomposition data also confirm the presence of coordination water in all complexes composition. The corresponding deformation band, assigned to $\delta(\text{H}_2\text{O})$, is overlapped by the IR strong bands from $1700-1600 \text{ cm}^{-1}$ zone.

The stretching vibration of N-H amide group of free L is a relative weak band and is partial overlapped by the $\nu(\text{CH})$ band. After coordination of the ligand L, the $\nu(\text{NH})$ band become total overlapped by the strong absorption of $\nu(\text{OH})_{(\text{H}_2\text{O})}$ band and partial overlapped by the $\nu(\text{CH})$ one for all complexes,

excepting the Cu(II) complex. The values of NH stretching vibration frequency decreased from 3115 cm^{-1} for $[\text{Mn}(\text{L})_2]\cdot 2\text{H}_2\text{O}$ to 3060 cm^{-1} for $[\text{Cu}(\text{L})_2]\cdot 2\text{H}_2\text{O}$ (Table 2) with the increasing of electronic density of the metal ion and the decreasing of a class character of Lewis acid. The shift of $\nu(\text{NH})$ of amide group indicates the increasing of covalent degree of N-M bond.

The C-H stretching vibration of methylene group generates relatively broadband in the $2900\text{--}3150\text{ cm}^{-1}$ region, that will partially hide the $\nu(\text{CH})$ multiple bands of the phenyl groups. The $\nu(\text{CH})$ frequency of methylene group shifts to high values (Table 1) after the coordination of the ligand as a consequence of the electronic density decreasing at the carbon atom due to the change of its hybridization state from partial sp^2 to sp^3 .

The spectra show a series of very weak intensity bands in the $2800\text{--}2200\text{ cm}^{-1}$ zone that are characteristic to the amino acid salts and can be attributed to the combination bands of deformation vibration by Fermi resonance (Nakamoto, 1986).

The spectral $1700\text{--}1300\text{ cm}^{-1}$ region is populated by many frequency values which complicates the assignment of the stretching vibration mode of carboxylate group by the $\nu(\text{C}=\text{O})_{\text{amide I}}$, $\nu(\text{C}=\text{C})_{\text{phenyl}}$, $\nu(\text{C}-\text{N})_{\text{amide II}}$, $\delta(\text{NH})$, $\delta(\text{CH})$ modes. The very strong band around 1645 cm^{-1} in spectra of coordination compounds can be assigned to the asymmetric stretching vibration of the carboxylate group which is overlapped with the $\delta(\text{NH})$.

The synthesized complexes also show another strong or medium intensity bands at 1409 , 1407 , 1406 and 1412 cm^{-1} that can be assigned to the symmetric vibration of the COO^- group that partial overlaps with CH bending frequency. The COO^- can act as monodentate or bidentate ligand, and the frequency of separation between $\nu_{\text{as}}(\text{COO})$ and $\nu_{\text{s}}(\text{COO})$ ($\Delta\nu(\text{COO})$) is a mode to distinct between the two binding states (Mann *et al.*, 1995). The $\Delta\nu(\text{COO})$ values for all coordination compounds are 238 , 232 , 235 and 227 cm^{-1} , fact that suggest a monodentate interaction of carboxylate group with metal ion.

The influence of the metal cations on the amidic II C=O group electronic density is almost the same. This means that the ketonic bond becomes weaker and the amidic bond stronger.

The most important changes after ligand coordination take place within the range of $1000\text{--}400\text{ cm}^{-1}$ (Fig. 1). The spectra display the bands with different intensities. The position of the M-ligand vibrations is difficult to establish, but $\nu(\text{M}-\text{N})$ appears at higher energy than $\nu(\text{M}-\text{O})$.

3.1.3. DR Electronic Spectra

The electronic spectra of the ligand L and the four synthesized complexes are presented in Fig. 3. The spectral components are summarized in Table 3.

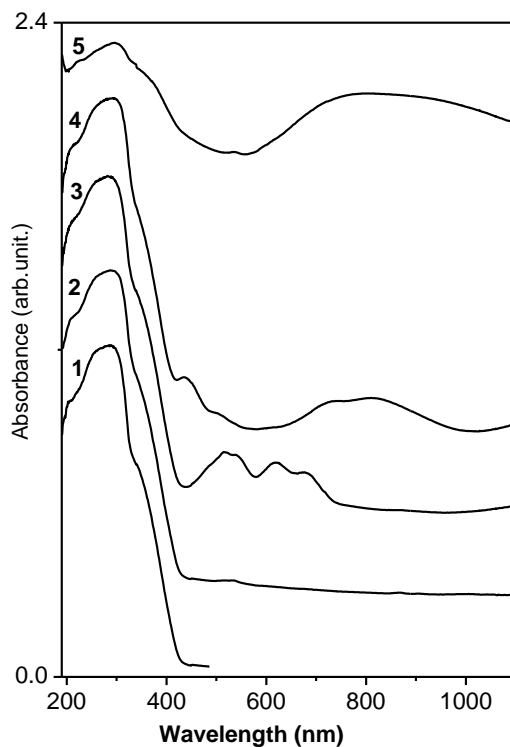


Fig. 3 – Electronic DR spectra of the (1)L, (2)[Mn(L)₂] \cdot 2H₂O, (3)[Co(L)₂] \cdot 2H₂O, (4)[Ni(L)₂] \cdot 2H₂O and (5)[Cu(L)₂] \cdot 2H₂O.

Table 3

The DR Spectral Data (λ , nm), Dq (cm⁻¹) and B (cm⁻¹) Crystal Field Parameters for N-p-Nitrobenzoyl-D-L-Phenylglycine and its Me(II) Derivatives Compounds

Compound	Ligand-ligand				Charge transfer	d-d				Dq [cm ⁻¹]	B* [cm ⁻¹]
	201	259	300	347							
(1)	201	259	300	347							
(2)	201	265	307	355	–	494	533			348	790
(3)	201	266	304	348	488	554	615	682	1145	869	630
(4)	198	267	308	351	443	496	745	881	1121	968	642
(5)	<190	227	294	355	693		779	912	1045	–	–

*Racah parameter

(1) L, (2) [Mn(L)₂] \cdot 2H₂O, (3) [Co(L)₂] \cdot 2H₂O, (4) [Ni(L)₂] \cdot 2H₂O and (5) [Cu(L)₂] \cdot 2H₂O

The electronic spectrum of free ligand appears as an intense, asymmetric band in the UV region. After deconvolution, four absorption bands corresponding to 201, 259, 300 and 347 nm, respectively were identified. These transition bands were assigned to the n- π^* and π - π^* transitions, both types being split into two different components. Their transition energy depends on the

electronegativity of atoms and the auxochrome groups effect: $(\downarrow(n\downarrow N - \pi^{\uparrow*})) = 28818 \text{ cm}^{-1}$ (347 nm), $(\downarrow(n\downarrow O - \pi^{\uparrow*})) = 3333 \text{ cm}^{-1}$ (300 nm), $(\downarrow(\pi\downarrow C - \text{-phenil}) - \pi^{\uparrow*}) = 38610 \text{ cm}^{-1}$ (259 nm) and $(\downarrow(\pi\downarrow C - \text{-phenil}) - \pi^{\uparrow*}) = 49751 \text{ cm}^{-1}$ (201 nm). Absorption spectra of Mn(II), Co(II), Ni(II) and Cu(II) N-p-nitrobenzoyl-D-L-phenylglycines show the same number of bands for each complexes (Table 3). The shift of absorbance to the higher values of λ_m in all of the complexes is attributed to the complexation behaviour of L ligand towards metal cations. The second $\pi_{C\text{-phenyl}}-\pi^*$ transition is less influenced by the coordination which indicates that it does not belong to the p-nitrobenzoyl ring.

The structure of M(II) complexes consists in a monomer unit in which coordination sphere of the M(II) is formatted by two oxygen atoms of carboxyl group, two amidic nitrogen atoms and two aqua ligands (Fig. 1). The interpretation of all spectra can be done in the octahedral symmetry, the structure of the complexes being generated by the tetragonal distorted O_h symmetry (Titiš *et al.*, 2012).

In the range 400 – 600 nm, the $[\text{Mn}(\text{L})_2] \cdot 2\text{H}_2\text{O}$ exhibits two weak d-d bands attributed to ${}^6\text{A}_{1g} - {}^4\text{T}_{1g}(\text{G})$ (566 nm) and ${}^6\text{A}_{1g} - {}^4\text{T}_{2g}(\text{G})$ (438 nm) forbidden transitions (Table 2). The estimation of the crystal field strength for this compound is $Dq = 348 \text{ cm}^{-1}$ and $B = 790 \text{ cm}^{-1}$ indicating that the Mn(II) coordinative compound corresponds to the typical high spin complexes.

The spectra of Co(II), Ni(II) and Cu(II) complexes are typical for distorted octahedral coordination symmetry due to non-equivalent donor atoms of the ligand, steric hindrance and less to the Jahn-Teller effect.

For $[\text{Co}(\text{L})_2] \cdot 2\text{H}_2\text{O}$ four d-d transition bands at 1145 nm, 682, 615 and 554 nm, respectively were identified. The transitions can be assigned to ${}^4\text{E}_{2g}({}^4\text{T}_{2g}) - {}^4\text{A}_{2g}({}^4\text{T}_{1g}({}^4\text{F}))$, $({}^4\text{E}_{2g}({}^4\text{T}_{1g}({}^4\text{F})) - {}^4\text{A}_{2g})$ are $> 1150 \text{ nm}$, ${}^4\text{B}_{2g}({}^4\text{T}_{2g}) - {}^4\text{A}_{2g}$, ${}^4\text{B}_{1g}({}^4\text{A}_{2g}({}^4\text{F})) - {}^4\text{A}_{2g}$ and ${}^4\text{E}_g({}^4\text{T}_{1g}({}^4\text{P})) - {}^4\text{A}_{2g}$. The intensity of electronic transition bands and the gap between them allows the distinction between pseudo-square planar and octahedral symmetry of coordinative centre.

The Gaussian curve fittings of original DR spectrum of $[\text{Ni}^{\text{II}}(\text{L})_2(\text{H}_2\text{O})_2]$ are included in Table 3. The result of deconvolution is typical for a distorted octahedral Ni(II)- d^8 coordinative compounds. The λ_{d-d} determined correspond to ${}^3\text{T}_{2g}(\text{F}) - {}^3\text{A}_{2g}$ (1121 nm), ${}^3\text{T}_{1g}(\text{F}) - {}^3\text{A}_{2g}$ (881 nm), ${}^3\text{T}_{1g}(\text{P}) - {}^3\text{A}_{2g}$ (496 nm) spin-allowed transitions and ${}^1\text{E}_g - {}^3\text{A}_{2g}$ spin-forbidden transition. The higher energy states interact more with the larger and more with the polarisable N-donor atom than with the oxygen atom of L ligand. This is equivalent with a vibronically induced electronic transition of all four band transitions and a tetragonal distortion in the excited states.

For $[\text{Co}(\text{L})_2] \cdot 2\text{H}_2\text{O}$ and $[\text{Ni}(\text{L})_2] \cdot 2\text{H}_2\text{O}$ complexes the Dq and B values of crystal field parameters (Table 4) indicate an increase of the strength of ligand field and of the covalent character of metal-ligand bonds, respectively, compared with Mn(II) spectral data.

Electronic DR spectrum of Cu(II) – d^9 complex presents a strong and broad asymmetric band in the near-IR – Vis region. The broad band is

characteristic for distorted octahedral $[\text{Cu}(\text{L})_2] \cdot 2\text{H}_2\text{O}$ complexes to chromophore plane and spin-orbital coupling coefficient of Cu(II), which is higher than 800 cm^{-1} . The number and energy of d-d electronic transitions of Cu(II) are influenced by the polarization of the Cu-donor atom bonds (Parajón-Costa and Baran, 2012). As a consequence, the band is an envelope that resulted from partial overlapping of free identified electronic transition bands (Table 2) derived from tetragonal splitting of ${}^2t_{2g}$ and 2e_g orbital energy levels: $d_{z^2} \rightarrow d_{x^2-y^2}$, $d_{xy}, d_{xz} \rightarrow d_{x^2-y^2}$ and $d_{yz} \rightarrow d_{x^2-y^2}$.

The bands centred at 448, 443 and 693 nm was attributed to the $M(d_{x^2-y^2}) - L(\pi^*)$ charge transfer transitions, where M is Co(II), Ni(II) and Cu(II), respectively.

These observation sustain that N forms with M(II) a bond with higher covalent degree than oxygen, according with Lewis basic hardness theory of donor-atoms. The shift of $n_N - \pi^*$ transition is influenced by the compatibility between N-donor ligand and M(II), and by the electronic and steric effects of the substitute groups of organic ligand.

3.1.4. ESR Spectroscopy

The spectrochemical scission factor (g) and the number of impair electrons for each central ion was calculated based on literature (Bhave and Kharat, 1981) according to the following relation:

$$N_x = N_e \frac{(I_x H_{\max}^2)_x}{(I_e H_{\max}^2)_c} \quad (1)$$

where: N_x and N_e represents the number of impair electrons of the studied sample and of the standard sample, N_e has the value $0.281 \cdot 10^{20}$ impair electrons, $[\text{mL}^{-1}]$; I_x and I_e are the signal amplitudes for the analysed and respectively standard sample; $(H_{\max})_x$ and $(H_{\max})_e$ are the intensity values of the maximum magnetic field corresponding to the sample and to the standard.

The g factor was calculated according to the following relation:

$$g = g_e (H_x/H_e) \quad (2)$$

where: $g_e = 2.0055$ for the standard sample; H_x and H_e represent the magnetic field corresponding to the centre of the studied sample spectrum and respectively of the standard $H_e = 3216.9$ Gauss.

The above relations could be applied when both the spectra curves (analysed and standard) are the same type (Gauss or Lorentz). The g value is higher for the complexes with organic ligands and is correlated with the arrangement of the ligands around the central atom. Table 4 presents the g factor values for H_x and the number of the impair electrons corresponding to

each central atom. It can be observed that all complexes are paramagnetic and with high spin.

Table 4
ESR Parameters for Me(II) with N-p-Nitrobenzoyl-D-L-Phenylglycine (L)
Coordination Derivatives Compounds

Compound	<i>g</i>	H_x	Number of impair electrons / central ion
[Mn(L) ₂] \cdot 2H ₂ O	2.0305	3257.00	4.89
[Co(L) ₂] \cdot 2H ₂ O	2.0198	3239.70	2.91
[Ni(L) ₂] \cdot 2H ₂ O	2.0188	3229.90	1.92
[Cu(L) ₂] \cdot 2H ₂ O	2.0242	3214.50	0.96

3.1.5. X-ray Diffraction

Table 5 presents the results of X-ray interpretation.

Table 5
Elementary Cell Parameters of (1) L, (2) [Mn(L)₂] \cdot 2H₂O, (3) [Co(L)₂] \cdot 2H₂O, (4) [Ni(L)₂] \cdot 2H₂O and (5) [Cu(L)₂] \cdot 2H₂O

Parameters	(1)	(2)	(3)	(4)	(5)
<i>a</i> (Å)	13.1798	8.6233	15.7603	15.0955	6.7227
<i>b</i> (Å)	9.1906	13.9393	7.3370	6.0463	11.5693
<i>c</i> (Å)	6.3646	6.9489	6.6340	8.9904	18.4825
α (°)	92.2440	90	90	67.9950	38.6109
β (°)	111.7200	95.0030	92.1270	95.4160	55.0371
γ (°)	110.7040	90	90	95.1840	65.6129
<i>V</i> (Å) ³	647.7680	832.09	766.5800	755.5200	743.2300
Sistem	<i>Ortorombic</i>	<i>monoclinic</i>	<i>monoclinic</i>	<i>triclinic</i>	<i>triclinic</i>

(L) = N-p-nitrobenzoyl-D-L-phenylglycine

All complexes have one side (in which are positioned probably the water molecules) of polyhedron crystallization smaller than the other two. Also, the elementary cell volume of all coordination compounds is higher than the volume of the elementary cell ligand, due to the different nature of the forces that help maintain lattice (H-O_{carboxylate} bonds for ligand and dipolar for complex combinations). The crystallization system of the Cu(II) compound differs to the other compounds due to higher volume of the copper ion compared to the other divalent ions.

Based on the above presented data, the assigned structure of the complex combinations is presented in Fig. 4.

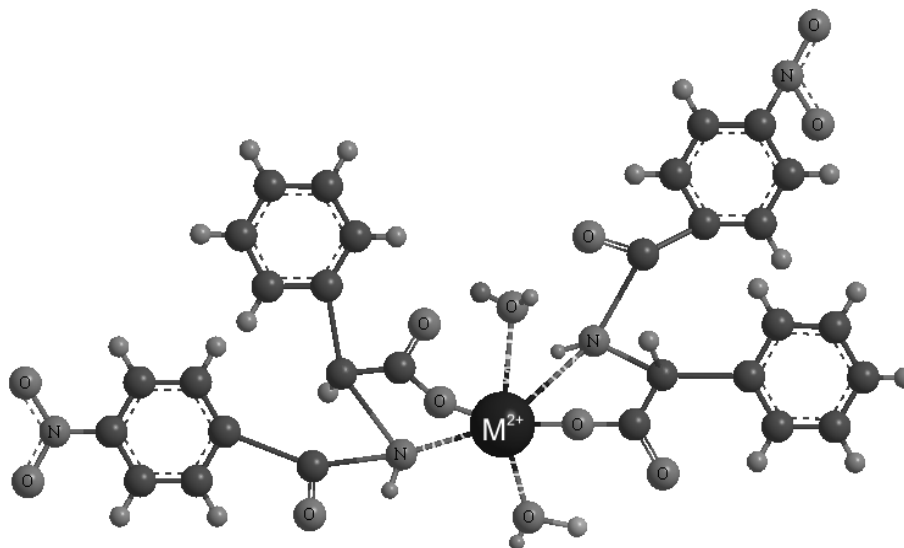
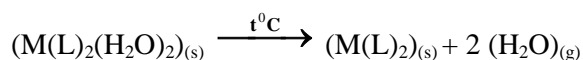


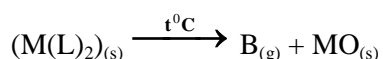
Fig. 4 – Structure of the complex combinations type: $M [(L)_2(H_2O)_2]$.

3.1.6. Thermal Analysis

In a first stage occurs the loss of coordination water molecules:



In the second oxidation step occurs the various fragments broken from the organic ligand:



where M is Mn, Co, Ni, Cu and B is a mixture of CO_2 , NO_2 and H_2O .

The main parameters of the thermal decomposition process, calculated by the method of Freeman – Carroll (1958), are presented in Table 6.

All the complexes decompose into three stages, except the $Ni(L)_2(H_2O)_2$ compound. As mentioned above, in the first stage the adsorbed and the coordination water is lost. In the second stage occurs the chemical bonds breaking between C (1), N (1) and the oxidation fragment, due to inductive and electromere effects induced by the presence of the metal with low electronegativity (Fig. 5), In the third stage is produced a complete break with the formation of metal oxide.

Table 6
Thermal Decomposition Process Parameters of (1) L, (2) [Mn(L)₂]·2H₂O, (3) [Co(L)₂]·2H₂O, (4) [Ni(L)₂]·2H₂O and (5) [Cu(L)₂]·2H₂O

Stage	Parameters	(1)	(2)	(3)	(4)	(5)
1	A	$1.47 \cdot 10^{20}$	$6.55 \cdot 10^{14}$	$5.68 \cdot 10^{18}$	$6.58 \cdot 10^{15}$	$1.32 \cdot 10^{15}$
	Ea/kJ·mol ⁻¹	207.82	72.35	49.84	34.34	35.53
	n	1.08	1.163	0.87	0.14	0.63
	Ti°C	201.4	42.5	42.5	82.5	89
	initial mg	2.6680	4.8050	2.9938	4.8319	3.4362
	loss%*	33.79	5.24/5.91	5.21/6.30	5.21/5.58	5.17/6.05
2	A	A continuous loss of 36.59%	$4.88 \cdot 10^{16}$	$1.10 \cdot 10^{15}$	$1.85 \cdot 10^{18}$	$1.10 \cdot 10^{15}$
	Ea/kJ·mol ⁻¹		72.55	75.77	77.32	75.07
	n		0.61	0.41	0.62	0.64
	Ti°C		147.5	130	124	182
	Residue %		48.45	45.92	38.92	45.23
3	A	$1.25 \cdot 10^{17}$	$9.04 \cdot 10^{18}$	$1.12 \cdot 10^{20}$	$3.00 \cdot 10^{20}$	$1.60 \cdot 10^{18}$
	Ea/kJ·mol ⁻¹	120.13	138.63	154.19	281.88	140.39
	n	0.91	0.62	0.76	1.02	0.67
	Ti°C	360.91	474	421.6	340	381
	loss%	28.57	35.67	37.38	22.76	37.45
4	A				$3.43 \cdot 10^{16}$	
	Ea/kJ·mol ⁻¹				134.33	
	n				1.25	
	Ti°C				436	
	loss%				22.83	
Final residue %**		1.05	10.03/9.97	10.87/10.4	10.83/9.91	11.43/11.27

* theoretical for M[(L)₂(H₂O)₂] → M[(L)₂] / practical

** theoretical M[(L)₂(H₂O)₂] → MO / practical

(L) = N-p-nitrobenzoyl-D-L-phenylglycine

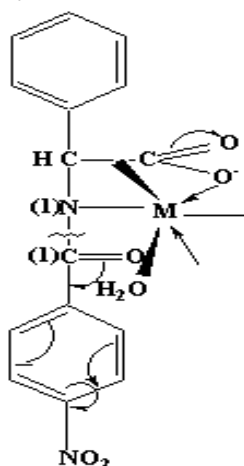


Fig. 5 – Inductive and electromere effects in the [M(L)₂].

In the case of the Ni (II) complex, decomposition occurs in four stages, the first one involving the loss of water molecules while the second is involving the loss of other similar compounds. The stages 3 and 4 are different, involving the breaking of organic fragments that occurs randomly.

In the case of the ligand free of the metal influence, decomposition takes place in two stages. In the first stage, the two benzene cycles will break due to oxidation inside organic fragment on the top of C (1), and -HN-HC-COOH, (theoretical loss of almost 33.79%, 32.14%), followed in a second stage, by the breakage and oxidation of the benzene cycles into a continuous phase, a much better-defined phase that will allow calculation of the kinetic parameters.

3.2. Biological Activity

3.2.1. Toxicity Analysis

The determination of the dose that kills 50% of the experimental animals (LD_{50}) represents an indispensable test for the characterization of a new (biological active) synthesized compound (Domer, 1971).

The gradual testing of toxicity was performed, by determining LD_{50} for the derivatives compounds of Mn, Co, Ni, and Cu with N-p-nitrobenzoyl-D-L-phenylglycine.

From the data presented in Table 7 can be observed that all tested compounds presented low toxicity. Among them, the compound 5, $Cu[(L)_2(H_2O)_2]$, showed the lowest toxic potential, close to that of the ligand. This observation is similar with the previous literature data (Moise *et al.*, 2008, Gravatt *et al.*, 1994; Moise *et al.*, 2009), according to which the use of N-acylated amino acids for different combinations will positively influence the toxicity degree.

Table 7

The Toxicity of (1) L, (2) $[Mn(L)_2] \cdot 2H_2O$, (3) $[Co(L)_2] \cdot 2H_2O$, (4) $[Ni(L)_2] \cdot 2H_2O$ and (5) $[Cu(L)_2] \cdot 2H_2O$

Compound	LD_{50} [mg/kg body]
(1)	6228
(2)	6118
(3)	6012
(4)	6053
(5)	6157

(L) = N-p-nitrobenzoyl-D-L-phenylglycine

3.2.2. Antibacterial and Antifungal Activity

Screening test results of ligand and synthesized complexes against various pathogenic bacteria and fungi species by using the agar well diffusion and the tube diffusion methods (Choudhary and Thomsen, 2001; Rattan, 1999) are given in Tables 8 and 9.

Table 8
Antibacterial Activity of (1) L, (2) $[Mn(L)_2] \cdot 2H_2O$, (3) $[Co(L)_2] \cdot 2H_2O$, (4) $[Ni(L)_2] \cdot 2H_2O$ and (5) $[Cu(L)_2] \cdot 2H_2O$

Bacteria	Zone of inhibition [mm]				
	(2)	(3)	(4)	(5)	(1)
<i>E. coli</i>	6	8	5	5	5
<i>B. subtilis</i>	21	24	14	18	12
<i>St. aureus</i>	9	11	7	7	6
<i>P. aeruginosa</i>	23	26	13	19	12

(L) = N-p-nitrobenzoyl-D-L-phenylglycine

All synthesized compounds showed significant antibacterial activity against the tested bacteria. The antimicrobial activity of N-p-nitrobenzoyl-D-L-phenylglycine derivatives has been found to decrease in the following order: Ni > Cu > Mn > Co. All screened compounds were more active against *B. subtilis* and *P. aeruginosa* than against *E. coli* and *St. aureus*. The ligand was found to be less active against the tested bacteria, but has an important role in determining the degree of the activity of the synthesized compounds.

Table 9
Antifungal Activity of (1) L, (2) $[Mn(L)_2] \cdot 2H_2O$, (3) $[Co(L)_2] \cdot 2H_2O$, (4) $[Ni(L)_2] \cdot 2H_2O$ and (5) $[Cu(L)_2] \cdot 2H_2O$

Fungus	Percent of growth inhibition [%]				
	(2)	(3)	(4)	(5)	(1)
<i>C. albicans</i>	43.6	33.1	14.8	54.3	13.2
<i>A. flavus</i>	5.2	3.8	2.4	8.2	1.5

(L) = N-p-nitrobenzoyl-D-L-phenylglycine

The antifungal activity of N-p-nitrobenzoyl-D-L-phenylglycine derivatives showed that the $Cu[(L)_2(H_2O)_2]$ is more active than the Mn, Ni, Co compounds. All the compounds were more active against *Candida albicans* than against *Aspergillus flavus*. The ligand also exhibited good activity, but only against *Candida albicans*. Thus, the activity of the synthesized compounds against the tested fungus species was observed to decrease in the following order: Cu > Mn > Co > Ni.

4. Conclusions

Four new compounds of Mn, Co, Ni, Cu with N-p-nitrobenzoyl-D-L-phenylglycine were synthesized and analyzed by various physicochemical methods in order to establish their structure.

All synthesized compounds presented low toxicity and especially Cu[(L)₂(H₂O)₂] revealed the lowest toxic potential, close to that of the ligand.

The N-p-nitrobenzoyl-D-L-phenylglycine derivatives showed significant antibacterial activity against the tested bacteria, the most effective being Co[(L)₂(H₂O)₂] against *B. subtilis* and *P. aeruginosa*.

All synthesized compounds presented moderate toxicity against the tested fungi, only Cu[(L)₂(H₂O)₂] proved a significantly growth inhibition against *C. albicans* (54.3%).

REFERENCES

- Bhave N.S., Kharat R.B., *Synthesis, Spectral and Magnetic Studies of Co-Ordination Polymers of Co(II), Ni(II), Cu(II) and Pd(II) with 2, 6-Dimercapto-4-Amino-1, 3, 5-Triazine (DAT)*, Journal of Inorganic and Nuclear Chemistry, **43**, 2, 414-416 (1981).
- Boxall A.B., Johnson P., Smith E.J., Sinclair C.J., Stutt E., Levy L.S., *Uptake of Veterinary Medicines from Soils into Plants*, Journal of Agricultural and Food Chemistry, **54**, 6, 2288-2297 (2006).
- Chen H., Li Z., Han Y., *Synthesis and Fungicidal Activity Against Rhizoctonia Solani of 2-Alkyl (Alkylthio)-5-Pyrazolyl-1, 3, 4-Oxadiazoles (Thiadiazoles)*, Journal of Agricultural and Food Chemistry, **48**, 11, 5312-5315 (2000).
- Choudhary M.I., Thomsen W.J., *Bioassay Techniques for Drug Development*, Taylor & Francis (2001).
- Domer F.R., *Animal Experiments in Pharmacological Analysis*, Springfield, III, Thomas, 283-297 (1971).
- Erol K., Sahin M.F., *Synthesis and Antinociceptive Activity of [(2-Oxobenzothiazolin-3-Yl) Methyl]-4-Alkyl/Aryl-1, 2, 4-Triazoline-5-Thiones*, Archiv Der Pharmazie, **334**, 8-9, 279-283 (2001).
- Freeman E.S., Carroll B., *The Application of Thermoanalytical Techniques to Reaction Kinetics: The Thermogravimetric Evaluation of the Kinetics of the Decomposition of Calcium Oxalate Monohydrate*, The Journal of Physical Chemistry, **62**, 4, 394-397 (1958).
- Gravatt G.L., Baguley B.C., Wilson W.R., Denny W.A., *DNA-Directed Alkylating Agents. 6. Synthesis and Antitumor Activity of DNA Minor Groove-Targeted Aniline Mustard Analogs of Pibenzimol (Hoechst 33258)*, Journal of Medicinal Chemistry, **37**, 25, 4338-4345 (1994).
- Gudasi K.B., Patil M.S., Vadavi R.S., Shenoy R.V., Patil S.A., Nethaji M., *X-Ray Crystal Structure of Phenylglycine Hydrazide: Synthesis and Spectroscopic Studies of its Transition Metal Complexes*, Spectrochimica Acta Part A: Molecular and Biomolecular Spectroscopy, **67**, 1, 172-177 (2007).

- Hamilton M.A., Russo R.C., Thurston R.V., *Trimmed Spearman-Kärber Method for Estimating Median Lethal Concentrations in Bioassays*, Environmental Science & Technology, **12**, 4, 714-719 (1977).
- Inomata Y., Shibata A., Yukawa Y., Takeuchi T., Moriwaki T., *The Metal Complexes of Amino Acids and their N-Substituted Derivatives–VII. The i.r. Spectra and Normal Coordinate Analyses of Bivalent Metal Complexes with N-Methylglycine and N-Phenylglycine*, Spectrochimica Acta Part A: Molecular Spectroscopy, **44**, 1, 97-107 (1988).
- Mann B.E., Clark S.J., Dillon K.B., *Spectroscopic Properties of Inorganic and Organometallic Compounds*, Vol. **28**, G. Davidson (Ed.), Royal Society of Chemistry (1995).
- Moise M., Șunel V., Profire L., Popa M., Desbrieres J., Peptu C., *Synthesis and Biological Activity of Some New 1, 3, 4-Thiadiazole and 1, 2, 4-Triazole Compounds Containing a Phenylalanine Moiety*, Molecules, **14**, 7, 2621-2631 (2009).
- Moise M., Șunel V., Profire L., Popa M., Lionte C., *Synthesis and Antimicrobial Activity of Some New (Sulfon-Amidophenyl)-Amide Derivatives of N-(4-Nitrobenzoyl)-Phenylglycine and N-(4-Nitrobenzoyl)-Phenylalanine*, Farmacia, **56**, 3, 283-289 (2008).
- Nakamoto K., *Infrared and Raman Spectra of Inorganic and Coordination Compounds*, John Wiley & Sons, Ltd. (1986).
- Parajón-Costa B.S., Baran E.J., *Vibrational and Electronic Spectra of [Cu(l-Ornithinato)₂Cl₂].2H₂O*, Spectrochimica Acta Part A: Molecular and Biomolecular Spectroscopy, **98**, 252-255 (2012).
- Pelagatti P., Bacchi A., Calbiani F., Carcelli M., Elviri L., Pelizzi C., Rogolino D., *Inverted Piano-Stool Dimers of Half-Sandwich Ru (II) Complexes with (R)-Phenylglycine Methyl ester and (S)-Phenylalanineamide: An X-Ray Structural Study and Preliminary Catalytic Results*, Journal of Organometallic Chemistry, **690**, 21, 4602-4610 (2005).
- Pintilie O., Moise M., Profire L., Șunel V., *Synthesis and Biological Activities of Some Beta-Lactamic Derivatives*, Farmacia, **54**, 5, 61 (2006).
- Pintilie O., Șunel V., Profire L., Pui A., *Synthesis and Antimicrobial Activity of Some New (Sulfonamidophenyl)-Amides of N-(m-Nitrobenzoyl)-D, L-Methionine*, Farmacia, **55**, 3, 345 (2007a).
- Pintilie O., Profire L., Șunel V., Popa M., Pui A., *Synthesis and Antimicrobial Activity of Some New 1, 3, 4-Thiadiazole and 1, 2, 4-Triazole Compounds Having a D, L-Methionine Moiety*, Molecules, **12**, 1, 103-113 (2007b).
- Rattan A., *Antifungal Susceptibility Testing*, Indian Journal of Medical Microbiology, **17**, 3, 125-128 (1999).
- Ryabov A.D., Polyakov V.A., Yatsimirsky A.K., *Some Complexes of Palladium (II) with C-Phenylglycine and its Derivatives. Cyclopalladation of N, N-Dimethyl-C-Phenylglycine Ethyl Ester*, Inorganica Chimica Acta, **91**, 1, 59-65 (1984).
- Salas Peregrin J.M., Colacio Rodriguez E., Suarez Varela J., Avila Roson J.C., *Synthesis, Characterization and Thermal Behaviour of Some N-2, 3-Dimethyl-Phenylglycine Compounds of Al(III), Mn(II), Fe(III), Y(III), Cd(II), La(III), Ce(III) and Pb(II)*, Thermochemica Acta, **95**, 1, 111-118 (1985).
- Sperry J.B., Wright D.L., *Furans, Thiophenes and Related Heterocycles in Drug Discovery*, Current Opinion in Drug Discovery & Development, **8**, 6, 723-740 (2005).

- Strohl W.R., *The Role of Natural Products in a Modern Drug Discovery Program*, Drug Discovery Today, **5**, 2, 39-41 (2000).
- Șunel V., Lionte C., Basu C., Chepte C., *New Antitumour Alkylating Compounds with N-[m-(Arylthiocarbamoyl)-Aminobenzoyl]-Asparagic Acids as Support*, Chem. Indian J., **2**, 1-6 (2005).
- Șunel V., Lionte C., Popa M., Pintilie O., Mungiu O.C., Telesman S., *Synthesis of New Methionine Derivatives for the Treatment of Paracetamol-Induced Hepatic Injury*, Eurasian Chem. Tech. J., **4**, 201-222 (2002).
- Șunel V., Popa M., Desbrières J., Profire L., Pintilie O., Lionte C., *New Di-(β -Chloroethyl)- α -Amides on N-(Meta-Acylaminobenzoyl)-D, L-Aminoacid Supports with Antitumoral Activity*, Molecules, **13**, 1, 177-189 (2008).
- Titiș J., Hudák J., Kožíšek J., Krutošiková A., Moncol J., Tarabová D., Boča R., *Structural, Spectral and Magnetic Properties of Carboxylato Cobalt (II) Complexes with Heterocyclic N-Donor Ligands: Reconstruction of Magnetic Parameters from Electronic Spectra*, Inorganica Chimica Acta, **388**, 106-113 (2012).
- Varvaresou A., Tsantili-Kakoulidou A., Siatra-Papastaikoudi T., Tiligada E., *Synthesis and Biological Evaluation of Indole Containing Derivatives of Thiosemicarbazide and their Cyclic 1, 2, 4-Triazole and 1, 3, 4-Thiadiazole Analogs*, Arzneimittel-Forschung, **50**, 1, 48-54 (2000).
- Wujec M., Pitucha M., Dobosz M., Kosikowska U., Malm A., *Synthesis and Potential Antimycotic Activity of 4-Substituted-3-(Thiophene-2-Yl-Methyl)- Δ 2-1, 2, 4-Triazoline-5-Thiones*, Acta Pharm, **54**, 251-260 (2004).
- Zou X.J., Lai L.H., Jin G.Y., Zhang Z.X., *Synthesis, Fungicidal Activity, and 3D-QSAR of Pyridazinone-Substituted 1, 3, 4-Oxadiazoles and 1, 3, 4-Thiadiazoles*, Journal of Agricultural and Food Chemistry, **50**, 13, 3757-3760 (2002).

SINTEZA, CHARACTERIZAREA ȘI EVALUAREA ACTIVITĂȚII
BIOLOGICE A UNOR COMPLEXȘI DIVALENȚI DE METALE TRANZIȚIONALE
CU N-p-NITROBENZOIL-D-L-FENILGLICINĂ

(Rezumat)

Lucrarea prezintă sinteza unor combinații complexe ale Mn(II), Co(II), Ni(II) și Cu(II) cu ligandul N-p-nitrobenzoil-D-L-fenilglicină (NBPG). Caracterizarea compușilor sintetizați menționați mai sus implică determinarea structurii prin analiza elementară, spectroscopia FTIR, difracția de raze X (XRD) și rezonanța electronică de spin (ESR). De asemenea, stabilitatea termică a fost evaluată prin descompunere termică. Datele experimentale arată că toți complexii Mn, Co, Ni și Cu cu N-p-nitrobenzoil-D-L-fenilglicinei prezintă structură cristalină, fiind cristalizați în sistem ortorombic și sunt stabili termic până la temperaturi peste 100°C. Rezultatele testelor de toxicitate efectuate pe șoareci au indicat faptul că valoarea cea mai mică a dozei letale o are complexul de Cu. Investigarea activității antibacteriene și antifungice a arătat că compusul Co[(L)₂(H₂O)₂] prezintă cele mai bune proprietăți antibacteriene în timp ce compusul Cu[(L)₂(H₂O)₂] prezintă cele mai bune proprietăți antifungice.